

# Diatom-inferred aquatic impacts of the mid-Holocene eruption of Mount Mazama, Oregon, USA

Joanne Egan<sup>a\*</sup>, Timothy E.H. Allott<sup>b</sup>, Jeffrey J. Blackford<sup>c</sup>

<sup>a</sup>Department of Geography, Edge Hill University, St. Helens Road, Ormskirk, Lancashire, L39 4QP, United Kingdom

<sup>b</sup>Department of Geography, School of Environment, Education and Development, University of Manchester, Oxford Road, Manchester, M13 9PL, United Kingdom

<sup>c</sup>Department of Geography, Environment and Earth Sciences, University of Hull, Cottingham Road, Hull, HU6 7RX, United Kingdom

(RECEIVED August 21, 2017; ACCEPTED June 8, 2018)

## Abstract

High-resolution diatom stratigraphies from mid-Holocene sediments taken from fringe and central locations in Moss Lake, a small lake in the foothills of the Cascade Range, Washington, have been analyzed to investigate the impacts (and duration) of tephra deposition on the aquatic ecosystem. Up to 50 mm of tephra was deposited from the climactic eruption of Mount Mazama 7958–7795 cal yr BP, with coincident changes in the aquatic ecosystem. The diatom response from both cores indicates a change in habitat type following blanket tephra deposition, with a decline in tycho planktonic *Fragilaria brevistriata* and *Staurosira venter* and epiphytic diatom taxa indicating a reduction in aquatic macrophyte abundance. Additionally, the central core shows an increase in tycho planktonic *Aulacoseira* taxa, interpreted as a response to increased silica availability following tephra deposition. Partial redundancy analysis, however, provides only limited evidence of direct effects from the tephra deposition, and only from the central core, but significant effects from underlying environmental changes associated with climatic and lake development processes. The analyses highlight the importance of duplicate analyses (fringe and central cores) and vigorous statistical analyses for the robust evaluation of aquatic ecosystem change.

**Keywords:** Tephra impact; Diatoms; Mazama; Redundancy analysis; Holocene; Volcano

## INTRODUCTION

Volcanic eruptions may have major impacts on ecosystems and, although the proximal impacts are generally well understood, the distal impacts of distal tephra deposition are not well-defined (see Payne and Egan, 2017 for a review). The “fine” to “very fine” (between <30 and 100  $\mu\text{m}$ ) class size of ash is of particular importance in this context, as they have the longest atmospheric residence times, travel the furthest distance, and carry the most toxic volatiles (Payne and Blackford, 2008), which makes them particularly hazardous to the environment (Rose and Durant, 2009). The impact of volcanic eruptions on climate and ecosystems can be detrimental. This can be through direct climatic perturbations (Mass and Portman, 1989; McCormick et al., 1995; Zielinski, 2000; Stoffel et al., 2015), though such effects usually last only 1–3 years (McCormick et al., 1995; Zdanowicz et al., 1999). It is the effects of tephra deposition on different

receiving environments that may have longer-term, decadal to centennial (Barker et al., 2000; Telford et al., 2004; Blackford et al., 2014; Egan et al., 2016) and even millennial (Bradbury et al., 2004) effects and are more ambiguous in nature. Focusing on the aquatic effects of tephra deposition, this paper aims to enhance our understanding of tephra impacts.

Egan et al. (2016) conducted a study on the terrestrial impacts of the tephra deposited by the Plinian eruption of Mount Mazama, Cascade Range, 7682–7584 cal yr BP (95.4% probability range; Egan et al., 2015). Mount Mazama ejected nearly 50 km<sup>3</sup> of rhyodacitic magma into the atmosphere (ten times as much as the 1980 eruption of Mount St. Helens), and deposited ash over an area of approximately 1.7  $\times 10^6$  km<sup>2</sup> (Zdanowicz et al., 1999) in a predominantly northeasterly direction (Fig. 1). Egan et al. (2016) reported a significant local impact on the terrestrial environment surrounding Moss Lake, Washington, with decreases in the open habitat vegetation. Building on the potential impacts from the Mazama tephra deposit here, we are now primarily interested in the nature and duration of the aquatic impacts, which Egan et al. (2016) did not address. Egan et al. (2016) highlighted

\*Corresponding author at: Department of Geography, Edge Hill University, St. Helens Road, Ormskirk, Lancashire, L39 4QP, United Kingdom. E-mail address: eganj@edgehill.ac.uk (J. Egan).

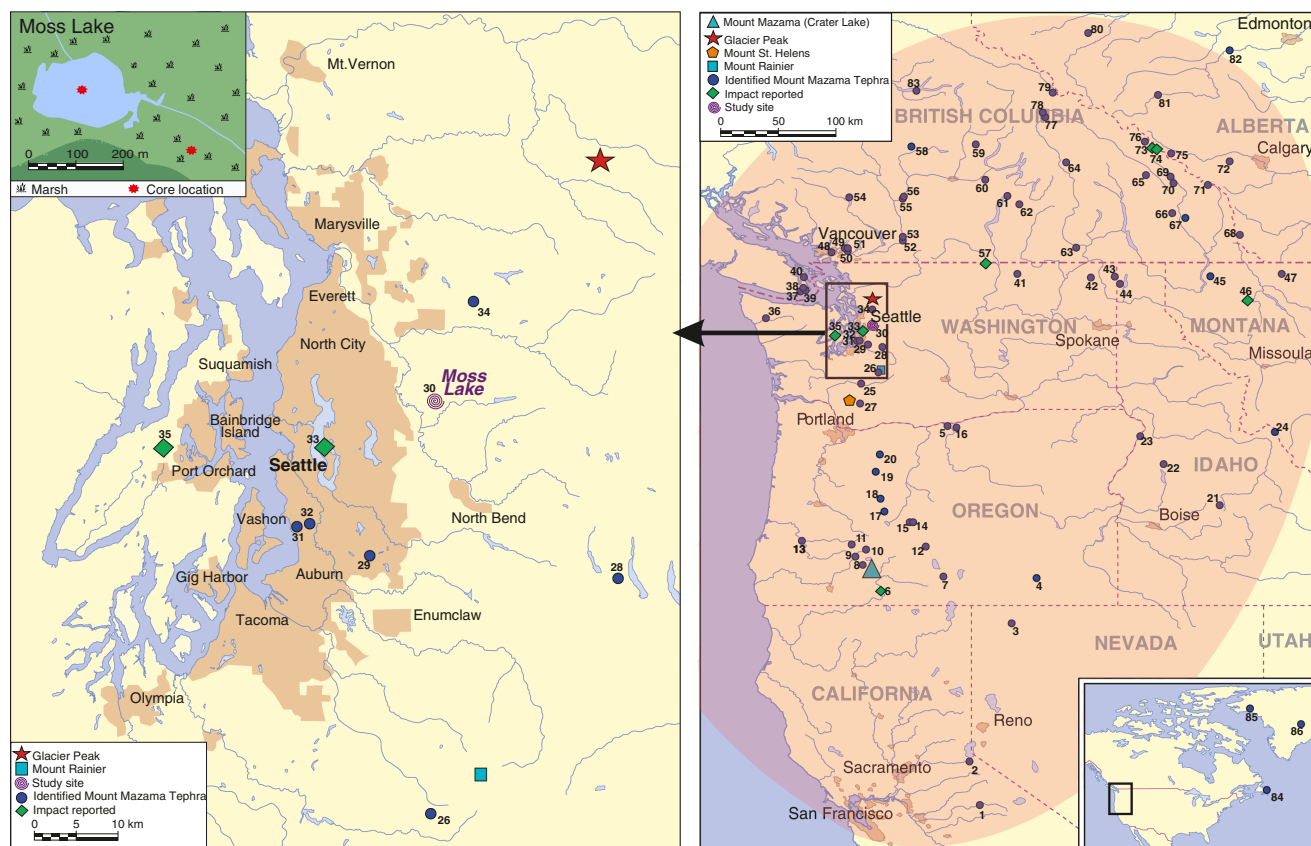


**Figure 1.** (color online) Extent of deposition from the Plinian eruption of Mount Mazama and sites where it has previously been identified. The elliptical shaded envelope in the map to the right shows the extent of recorded visible Mount Mazama tephra deposition. True tephra dispersal was much greater, with cryptotephra having been found as far as Newfoundland (Pyne-O'Donnell et al., 2012) and Greenland (Zdanowicz et al., 1999). The locations of Moss Lake, Mount Mazama, and Glacier Peak are also highlighted. The shading around cities indicates the size and distribution of major urban areas. A key is provided for the numbered sites in supplementary material Table 2.

the importance of multiple cores, as their analyses revealed a local terrestrial impact but no regional impact. Here we assess both shallow and deep cores from Moss Lake through the use of high-resolution diatom analyses to determine the physiochemical effects of tephra deposition on the aquatic environment.

Tephra can impact aquatic systems physically, biologically, and chemically. The direct input of tephra may instantly kill aquatic life, as tephra may get stuck in fish gills and can be toxic to aquatic organisms (Ayris and Delmelle, 2012; Lallement et al., 2016). Physically, tephra can make the water more turbid (Lallement et al., 2016), reduce light infiltration (Abella, 1988), alter drainage patterns and water flow (Lallement et al., 2016), and alter habitat availability with the death of aquatic plants reducing epiphytic species and newly deposited tephra allowing epipelagic algae to colonize (Telford et al., 2004). Such physical changes can have implications for the biology, as fish and algae can be displaced as their habitat is destroyed, and the changes in light penetration can reduce photosynthetic activity, thus altering oxygen levels in the water. Chemically, the aquatic system can be changed by increased concentrations of heavy metals (Power et al., 2011) or by decreasing the pH through the influx of associated sulfuric acid (Birks and Lotter, 1994).

Silica is also added to the aquatic system. Whilst this is an instant input, Telford et al., (2004) state that it dissolves slowly and, even when the tephra is deposited onto the lake bed, the silica will still be released, which provides a steady influx of silica to the aquatic system. Some diatom species are likely to be competitively advantaged and respond positively to the increased silica input (Telford et al., 2004). An additional effect of tephra deposition in lakes is that a thick tephra layer creates an impermeable barrier over the lake's sediment, preventing the regeneration of nutrients such as phosphorus (Barker et al., 2000, 2003). Tephra presents a physical barrier to the transport of phosphorus into the water column by preventing resuspension of the sediment by bioturbation and wave action, as well as a barrier to phosphorus diffusion, depending on its thickness. Any changes in the chemical status of the lake would impact the biological and thus physical characteristics of the aquatic system, as these three components are interconnected.

A recent study has assessed the aquatic impacts of tephra fallout from the rift zone eruption of the Puyehue-Cordón Caulle volcanic complex, Patagonia in 2011, and reported habitat loss, changes in morphology of the main channels, increases of turbidity, and a sharp decline in salmonid fish densities (Lallement et al., 2016). These impacts persisted for

30 months after the initial eruption, with some evidence that recovery is underway, but uncertainties exist as to whether the channels and their fish assemblages will ever return to the pre-impact conditions. Continuous monitoring in active volcanic terrains like this example is rare and few have the decadal durations required to record longer-term trends, thus much less is known about the long-term impacts on aquatic ecosystems.

Paleoenvironmental records have been used in several studies to successfully infer long-term impacts of volcanic eruptions and subsequent recovery. Diatoms are frequently used as a proxy for tephra impacts in lakes, as these algae are affected first due to their high sensitivity and rapid responses, and their preservation means that longer-term impacts can be assessed (Abella, 1988; Birks and Lotter, 1994; Barker et al., 2000; Colman et al., 2004; Telford et al., 2004). They are particularly useful for determining chemical and physical changes in the aquatic system.

Six studies have assessed the aquatic impacts of tephra deposition from Mount Mazama (Blinman et al., 1979; Abella, 1988; Hickman and Reasoner, 1994; Bradbury et al., 2004; Stone, 2005). The studies reported varying impacts, including a decrease of pH (Bradbury et al., 2004), increase of salinity (Heinrichs et al., 1999; Bradbury et al., 2004), a change in the Si:P ratio (Abella, 1988; Hickman and Reasoner, 1994), and changes in water chemistry that lasted nearly a millennium (Stone, 2005). Most of these lake systems are large in size and highly productive (Abella, 1988; Bradbury et al., 2004; Stone, 2005), and therefore not typical or representative of the majority of lakes in the Cascade region, which are smaller and nutrient poor (Hickman and Reasoner, 1994; Heinrichs et al., 1999). Evaluations are therefore needed from such systems, which may be more sensitive to disturbance. This study provides an assessment of the distal impacts of tephra deposition on the aquatic ecosystem of a small, oligotrophic lake system within the foothills of the Cascades.

## STUDY AREA

The Mazama tephra is of great stratigraphic importance, as the climactic eruption of Mount Mazama was a high magnitude event producing the most significant tephra fall of the Holocene in North America and it has been identified at Moss Lake. Moss Lake (47°41.60N, 121°50.81W; WGS 84 datum) is 500 km north of Crater Lake (the site of the Mount Mazama eruptions), allowing distal impacts to be assessed. Moss Lake is located in a mixed conifer forest within the Tolt river basin in King County in the Cascade foothills at an elevation of 158 m (Fig. 1). The lake has a diameter of approximately 200 m with a maximum depth of 4.5 m. Moss Lake resides in a shallow basin within a broad fluted basal till plain that was deposited during the Vashon Stade (~18,000–16,500 cal yr BP at the site; Porter and Swanson, 1998). This till sheet overlies glaciomarine drift and outwash deposits (Dragovich et al., 2002).

During the time of the deposition event, Moss Lake included an extensive shallow water system; today, the lake is surrounded by a reed swamp (see Fig. 1, inset in top left) underlain by lake sediments. This lake setting is ideal for the study, with stratigraphies from both a core from the fringing reed swamp, representative of the Holocene shallow-water system and potentially dominated by benthic taxa, as well as a deep-water core from the center of the lake, potentially with higher representation of planktonic and tychoplanktonic taxa. Moss Lake is a freshwater, oligotrophic system with a weakly acidic-neutral pH of 6 and low conductivity of 14–22  $\mu\text{S}/\text{cm}$ . Water chemistry analyses indicate the lake has a low concentration of calcium, suggesting that it has a low buffering capacity and may be sensitive to acid deposition from volcanic events (for present day water chemistry, see Supplementary Table 1). This study will add further detail to current knowledge regarding impacts of tephra deposition and, being in such close proximity to other major volcanoes such as Glacier Peak, Mount St. Helens, and Mount Rainier, it is essential that as much research is done in this area as possible.

## MATERIALS AND METHODS

### Core collection

To elucidate true volcanic impacts, cores were taken from the lake fringe (Moss Lake fringe, MLF) and a central part of the lake (Moss Lake central, MLC) representative of a shallow-water and deep-water lake system. MLC was collected from the deepest point of Moss lake, determined with an echosounder, using a modified Livingstone corer. A second core was extracted from the MLF using a Russian corer. The cores were placed in guttering, wrapped in cling film, and stored in the cold room (dark, 2–4°C) at the University of Manchester. As the focus of this paper is the impact of tephra deposition, analyses concentrate on sediments above and below the Mazama tephra deposit, not the whole Holocene record.

### Stratigraphic analyses and radiocarbon dating

Data reported here for the stratigraphy and chronology are taken from Egan et al. (2016), where further details of the methods can be found. To summarize, we measured the organic matter content, carbonates, particle size, and magnetic susceptibility. For the analyses here, we report the data from the samples taken every 5 mm above, below, and through the tephra layer (magnetic susceptibility was measured every 10 mm). Particle size analysis was carried out in order to assist with the determination of the tephra layer boundary in MLF, as it was not distinct. Samples were taken every 10 mm (every 5 mm through the tephra layer).

The Mazama tephra layer has previously been geochemically identified on the JEOL-JXA8600 electron microprobe at the Research Laboratory for Archaeology and the History of Art, University of Oxford (Egan et al., 2016).

AMS radiocarbon dates were obtained for both cores, as discussed in the previous work in Egan et al. (2016). Radiocarbon dating was carried out on bulk sediments, as there were no identifiable macrofossils or macrocharcoal fragments. The low sedimentary-carbonate content indicates that hard-water reservoir effects are unlikely. Originally, eight radiocarbon dates were obtained for MLC (Egan et al., 2016). Here, we present four of those ages that focus directly on the Mount Mazama deposit. Radiocarbon dates were calibrated to calendar years (cal yr BP) using OxCal v.4.2.4 (Bronk Ramsey, 2014), and the IntCal13 calibration curve (Reimer et al., 2013). A full chronology was determined with an age-depth model. We used a “P\_sequence” deposition model in OxCal v.4.2.4. To account for the 40-mm-thick tephra layer, representing instantaneous deposition, an “event free depth scale” was included (Staff et al., 2011). Three radiocarbon ages are reported for MLF. An age reversal was present, however, so an accurate chronology could not be determined.

### Diatom analysis

High-resolution samples (1-mm contiguous samples for MLF and 5-mm contiguous samples for MLC) were taken before and after the tephra layers. The age-depth model for MLC suggests these samples represent approximately 10–20 years. The high-resolution sampling was done by slicing the sediment with a scalpel and avoiding areas of tephra penetration outside of the primary tephra layer. Diatom preparation followed the standard procedure by Battarbee (1986) and followed Renberg’s (1990) recommendation of bulk preparation using a water-bath. Approximately 0.03 g of dry sediment was digested in 5 mL of 30% hydrogen peroxide; 1–2 drops of hydrochloric acid were added to eliminate any remaining hydrogen peroxide and carbonates. Samples were washed several times and weak ammonia was added on the final wash to keep clays in suspension and to prevent diatom clumping. Microspheres were added to determine diatom concentration (Battarbee and Kneen, 1982). The concentration of microspheres added was 2 mL of  $5.01 \times 10^6$  per 0.01 g dry weight of sediment. Samples were mounted on the microscope slide using Naphrax<sup>®</sup> and were identified and counted at 1000× magnification. Identification was through the website “Diatoms of the United States” (Spaulding, 2014) and identification keys (Krammer and Lange-Bertalot, 1991, 1999a, 1999b). At least 300 diatom frustules were counted.

Diatom diagrams presented here show the percentages of total frustules. The summary diagram is based on habitat preference determined primarily from “Diatoms of the United States” (Spaulding, 2014) and Kelly et al., (2005). Diatom zonation was used not only to assist with qualitative analyses, but also as a quantitative tool, as the zones determined represent significant changes in the assemblage. To determine statistically significant changes, optimal splitting by information content was used (Bennett, 1996), and the number of significant zones was determined through the use of the Broken-Stick model (Bennett, 1996). Diatom diagrams

and the zonation were created using Psimpoll v.4.27 (Bennett, 2007).

### Ordination and associated significance tests

Ordination was used to test for significant changes in the diatom record following the deposition of tephra, evaluating the significance of the impact of each tephra relative to, and independently from, additional environmental variables chosen to account for underlying environmental trends. Detrended correspondence analysis (DCA; Hill and Gauch, 1980) was used initially to estimate the length of the gradients in the biostratigraphical data sets (in standard deviation units). The diatom assemblages have short gradients (<1.7 SD), and consequently linear ordination methods were employed (Leps and Šmilauer, 2014). Principal component analysis (PCA; Orloci, 1966) was then used to describe the relationships between different diatom species and samples.

Partial redundancy analysis (RDA; Rao, 1964; ter Braak and Prentice, 1988), a constrained form of PCA, was used to determine how much of the variation is explained by the environmental variables and their significance. Log transformation and double centering of the samples and environmental variables were used to allow for the closed compositional disposition of the data. In order to test the significance of each environmental variable independent from the other two co-variables, time-series restricted Monte Carlo permutation tests used for stratigraphically ordered data (ter Braak and Šmilauer, 2012) were completed with 999 permutations. The significance test compares eigenvalues for the first RDA axes of the diatom assemblages. The statistical program used was Canoco v5 (ter Braak and Šmilauer, 2012).

The influence of three independent environmental variables (tephra, loss on ignition (LOI), and core depth) on the diatom data was evaluated using direct ordination (partial RDA). Observed changes in the diatom assemblages around the time of volcanic events may have been a response to tephra deposition. This effect is modelled as an exponential decay function through time (Lotter and Birks, 1993; Birks and Lotter, 1994; Barker et al., 2000; Lotter and Anderson, 2012). Prior to deposition of tephra, the tephra explanatory variable was given a value of 0. At the time of tephra deposition, the value for ash was given an arbitrary value of 100, and after deposition the value of ash decreased exponentially  $x^{-\alpha t}$ , where  $\alpha$  is the decay coefficient and  $t$  is sample time ( $f$ = depth) since tephra deposition. Three models (different decay coefficients) were used for the diatom assemblage from MLC to reflect different potential recovery times. Model 1 had a decay coefficient of 0.8 to reflect the longest recovery time of approximately 500 years, with most recovery having happened within approximately 200–250 years; model 2 had a decay coefficient of 0.5 to reflect medium duration or recovery of approximately 200 years, with most recovery having happened within approximately 100 years; and model 3 had a decay coefficient of 0.1 to reflect the shortest recovery time of approximately 80 years, with most recovery having happened within



approximately 20 years. An ongoing study in an alpine lake in Washington has found strong evidence that tephra from Mount Mazama exerted significant influence on sedimentation dynamics for up to 500 years post-deposition (Wershow, H.N., personal communication, 2015), thus the timeframes suggested by the models is realistic. For MLC, all models were used, as there was variation within the results. For MLF, however, there was little difference in the results, so the decay coefficient used for this assemblage was 0.5, model 2. LOI was the second environmental variable representing the inflow of exogenic mineral materials, which would be associated with low organic-matter content and local environmental change. LOI was corrected for tephra by interpolating values for the samples containing tephra, so there was no influence of the tephra itself on this variable. The third variable was depth, as a surrogate for age to represent directional change during the period of tephra deposition associated with climate change or successional processes.

## RESULTS

### Stratigraphy

A wider stratigraphy for MLC is reported in Egan et al., (2016). Figure 2 displays the stratigraphy of MLC around the time of Mazama tephra deposition (MLC-T324), the focus here. Figure 2 shows a shift from silty gyttja in sediment unit

MLCs-1 to organic peaty silt in MLCs-2. LOI decreases and drops to 5% upon the deposition of the Mazama tephra. Organic-matter content increases steadily after this in MLCs-2. Magnetic susceptibility increases upon tephra deposition from  $0.2 \times 10^{-7}$  SI to  $59 \times 10^{-7}$  SI. Carbonate content values are consistently below 0.01%. Figure 3 illustrates the MLF stratigraphy (again, a wider stratigraphy is presented in Egan et al. [2016]). Particle size analysis was used to determine the boundary of tephra deposition and shows a peak in coarse and fine sand between 158–153 cm, indicative of the tephra boundary. At the base of sediment unit MLFs-1, organic sandy silts dominate with low LOI ( $\sim 25\%$ ) and magnetic susceptibility values of  $3.5 \times 10^{-6}$  SI. Within the Mazama tephra deposit (MLF-T158) LOI further decreases to  $\sim 17\%$  and magnetic susceptibility peaks to  $94 \times 10^{-6}$  SI. In MLFs-2, silty peats develop with an increasing LOI from  $\sim 20$  to  $\sim 80\%$  and generally low magnetic susceptibility of  $1\text{--}7 \times 10^{-6}$  SI. A silt unit is present from 146–132 cm. There is a brief increase of magnetic susceptibility (to  $45 \times 10^{-6}$  SI) and particle size at around 120 cm, where there is a coarse sand deposit. Carbonate content values are consistently below 0.03%.

### Radiocarbon

The MLC sediment record extends back to the late Pleistocene, 16,294–12,789 cal yr BP, reported previously in Egan et al., (2016) and is well-constrained. The focus here,

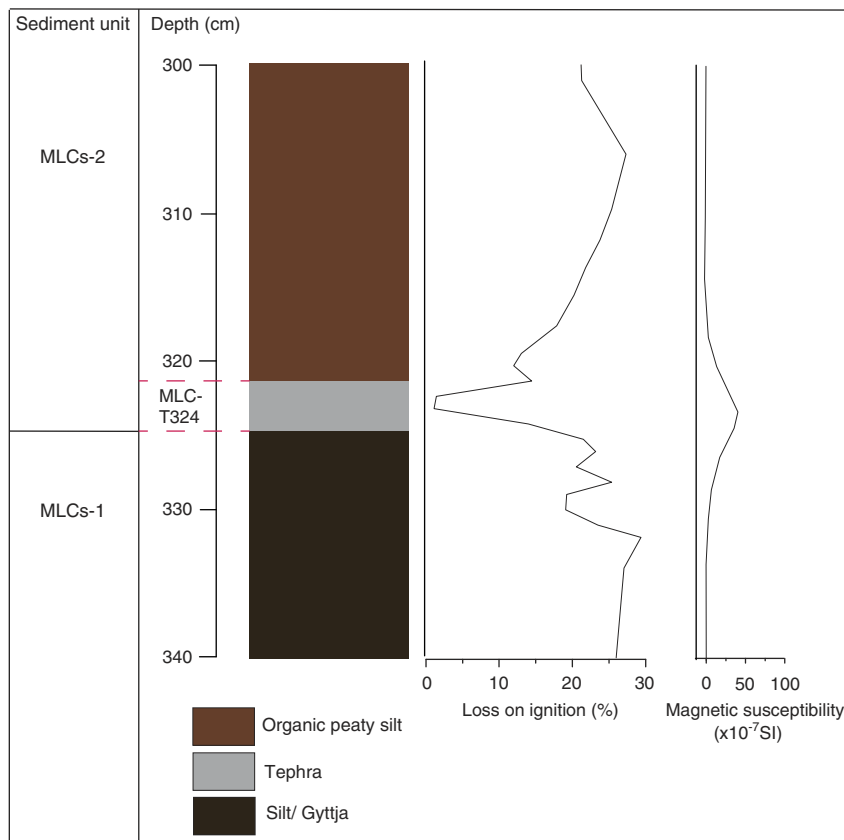


**Figure 2.** Lithology, % LOI, magnetic susceptibility, and carbonate content of Moss Lake central (MLC).

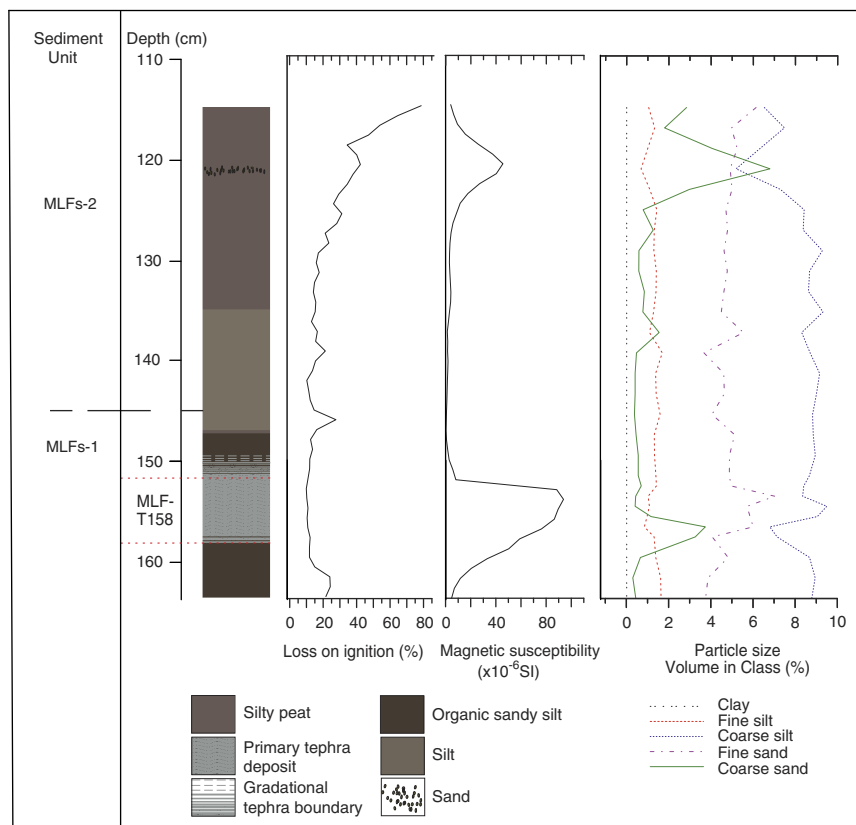


**Figure 3.** Lithology, % LOI, magnetic susceptibility, carbonate content, and particle size of Moss Lake fringe (MLF).

however, is on the aquatic impact of the Mazama tephra deposit. Thus, the record presented here spans the time period ~8400 to ~7100 cal yr BP (Table 1, Fig. 4). The three radiocarbon dates for MLF demonstrated an age reversal in the top two samples and was confirmed by re-analysis of the samples (Supplementary Table 3). The dates therefore cannot be used in the analyses but are provided to demonstrate that MLF-T158 is within the right time period, as the sediments below the tephra have a calibrated age range of 7958–7795 cal yr BP (95.4% probability range). Therefore, further up the core within the tephra layer, the age is likely to be younger and within the previously published age range of 7682–7584 cal yr BP (95.4% probability range; Egan et al., 2015).

### Diatoms

MLC has high proportions of planktonic *Discostella pseudostelligera* (up to 60%) and low proportions of epipelagic (~10%) and epiphytic (<5%) taxa. *Discostella pseudostelligera* is dominant throughout the assemblage. Figure 5 displays the diatom assemblage for MLC and Table 2 summarizes the main changes in the diatom assemblage around the time of Mazama tephra deposition. Three zones have been identified. The first zone (C1) includes the pre-tephra assemblage and the tephra deposit itself. The transition into the second zone (C2) starts above the tephra deposit at 320.8 cm and the third zone (C3) starts at 313.7 cm. The

**Table 1.** Conventional ( $^{14}\text{C}$  yr BP), calibrated (cal yr BP), and modelled (at 95.4% probability range) radiocarbon ages for MLC previously reported in Egan et al. (2016).

Lab no.	Depth (cm)	Material	Age ( $^{14}\text{C}$ years BP $\pm$ 1 SD)	Age range (cal yr BP $\pm$ 2 SD)	Modelled age range (cal yr BP 95.4% probability range)
SUERC-59476	305	Organic sediment	6330 $\pm$ 36	7410–7167	7286–7163
SUERC-59477	315	Organic sediment	6590 $\pm$ 38	7565–7430	7486–7424
SUERC-59478	321	Organic sediment directly above Mazama	6687 $\pm$ 39	7619–7480	7622–7531
Mazama <sup>a</sup>	324	–	–	7682–7584 <sup>b</sup>	–
SUERC-59479	345	Organic sediment	7430 $\pm$ 39	8344–8180	8351–8178

<sup>a</sup>Age range from Egan et al. (2015).

<sup>b</sup>Age range based on deposition model.

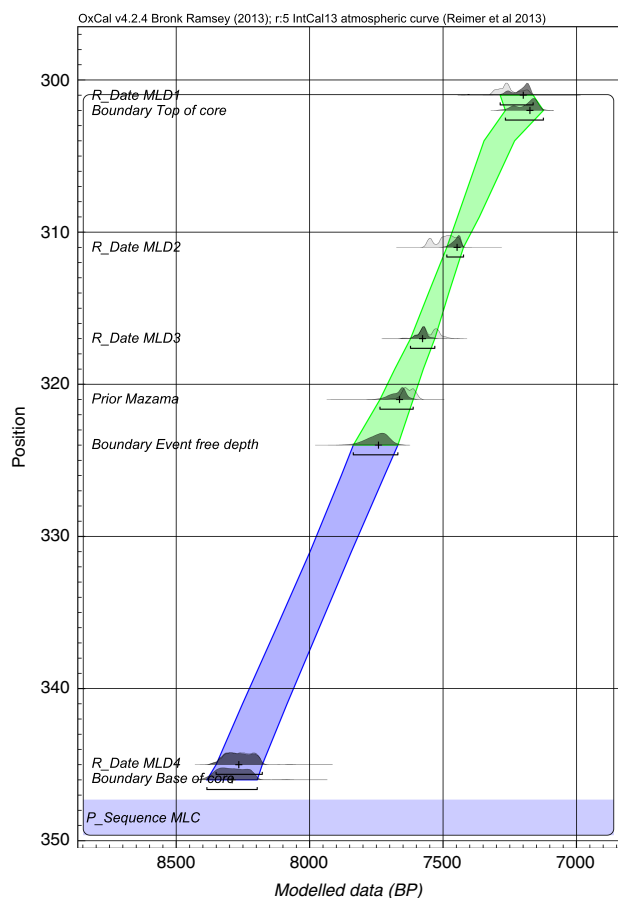


**Figure 4.** (color online) Bayesian age-depth (OxCal v.4.2; Bronk Ramsey, 2014) model for MLC derived from the comparison of the radiocarbon ages calibrated using the IntCal13 (Reimer, 2013) dataset.

zonation suggests tephra deposition from Mount Mazama caused marked change in the aquatic environment, with clear differences in the assemblages before and after tephra deposition. In zone C1, *Discostella pseudostelligera* increasingly dominates from 40% to 60%, and tycho planktonic species *Fragilaria brevistriata* and *Staurosira venter* decrease from 15 to <5% and 25 to <5% respectively. When tephra is deposited, *Aulacoseira* taxa increase by a small percentage (<5%) and *Fragilaria brevistriata* and *Staurosira venter* decrease further to <5%. In zone C2, *Discostella pseudostelligera* still dominates but decreases from 60 to 40%, whilst tycho planktonic taxa increase overall from 30 to 45%. Zone C3 consists of a higher abundance of *Discostella pseudostelligera* (up to 70%), *Aulacoseira* taxa (>20%), *Fragilaria brevistriata* (up to 20%), and *Staurosira venter* (up to 20%) than in zone C2.

MLF (Table 2, Fig. 6) has a very different assemblage to MLC, in particular lower proportions of planktonic *Discostella pseudostelligera* (<5%) and higher proportions of epipelagic (up to 50%) and epiphytic (up to 50%) taxa. The assemblage is dominated by epiphytic taxa throughout most of the profile, specifically *Eunotia soleirolii*, *Encyonema mesianum*, and *Gomphonema gracile*. Tycho planktonic taxa,

specifically *Aulacoseira lirata*, have a high abundance (up to 55%) before the tephra deposition event, and epipelagic taxa are high in abundance (up to 50%) after the tephra event, notably *Brachysira brebissonii* increasing from <5 to 20%. Two zones have been identified, and the split is during the time of Mazama tephra deposition, suggesting there was a marked assemblage change. Before tephra deposition in zone F1, epiphytic taxa dominate (up to 40%), in particular *Gomphonema gracile* and *Eunotia soleirolii* along with tycho planktonic *Aulacoseira lirata*, *Aulacoseira alpigena*, *Fragilaria brevistriata*, and *Staurosira venter*. Epipelagic taxa increase after tephra deposition from 20 to 50%. In zone F2, epipelagic species, especially *Brachysira brebissonii*, dominate. Tycho planktonic and epiphytic taxa are in lower abundance than in zone F1, decreasing from up to 50 to 10% and 50 to 40%, respectively.

## Ordination and significance tests (PCA and partial RDA)

### Principal Components Analysis

The gradients in both data sets for MLF and MLC had lengths of 1.1 and 0.7 SD units, respectively. These short gradient lengths show that there was restricted turn-over in the diatom data, as a standard deviation unit length of 4 would be indicative of complete species turnover (Lepš and Smilauer, 2014).

MLC has two important PCA gradients (Fig. 5): PCA axis 1 accounts for 26% of the variance and PCA axis 2 explains a further 21% of the variance. PCA axis 1 is associated with short-term variations in tycho planktonic taxa (Fig. 5), with a shift from positive to negative sample scores in zone C1, until Mazama tephra deposition in zone C2, where sample scores increase and become positive. In zone C3, sample scores return to values observed in zone C1. Positive sample scores are driven by *Aulacoseira crassipunctata* and *Nitzschia palea*. Negative sample scores are driven by *Staurosira venter* and *Fragilaria brevistriata*.

PCA axis 2 is more strongly related to the diatom response to tephra deposition, as there is a clear coherence between change in PCA axis 2 and the tephra deposition, specifically the responses of *Discostella pseudostelligera* and *Aulacoseira* taxa. Sample scores are weakly negative in zone C1 and become positive around the time of tephra deposition. In zone C2, sample scores are variable but positive, then decrease towards the top of the zone, and increase in zone C3, where sample scores fluctuate again. Positive sample scores are dominated by *Aulacoseira lirata* and *Aulacoseira alpigena*. The negative sample scores are dominated by *Discostella pseudostelligera* and *Tabellaria flocculosa*.

For MLF PCA, axis 1 accounts for 50.39% of the variance and represents the dominant gradient in the diatom data (Fig. 6). PCA axis 2 accounts for only a further 8% of the variance. Sample scores of PCA axis 1 are strong and positive in zone F1, then become weakly negative in zone F2 around the time of Mazama tephra deposition. After tephra

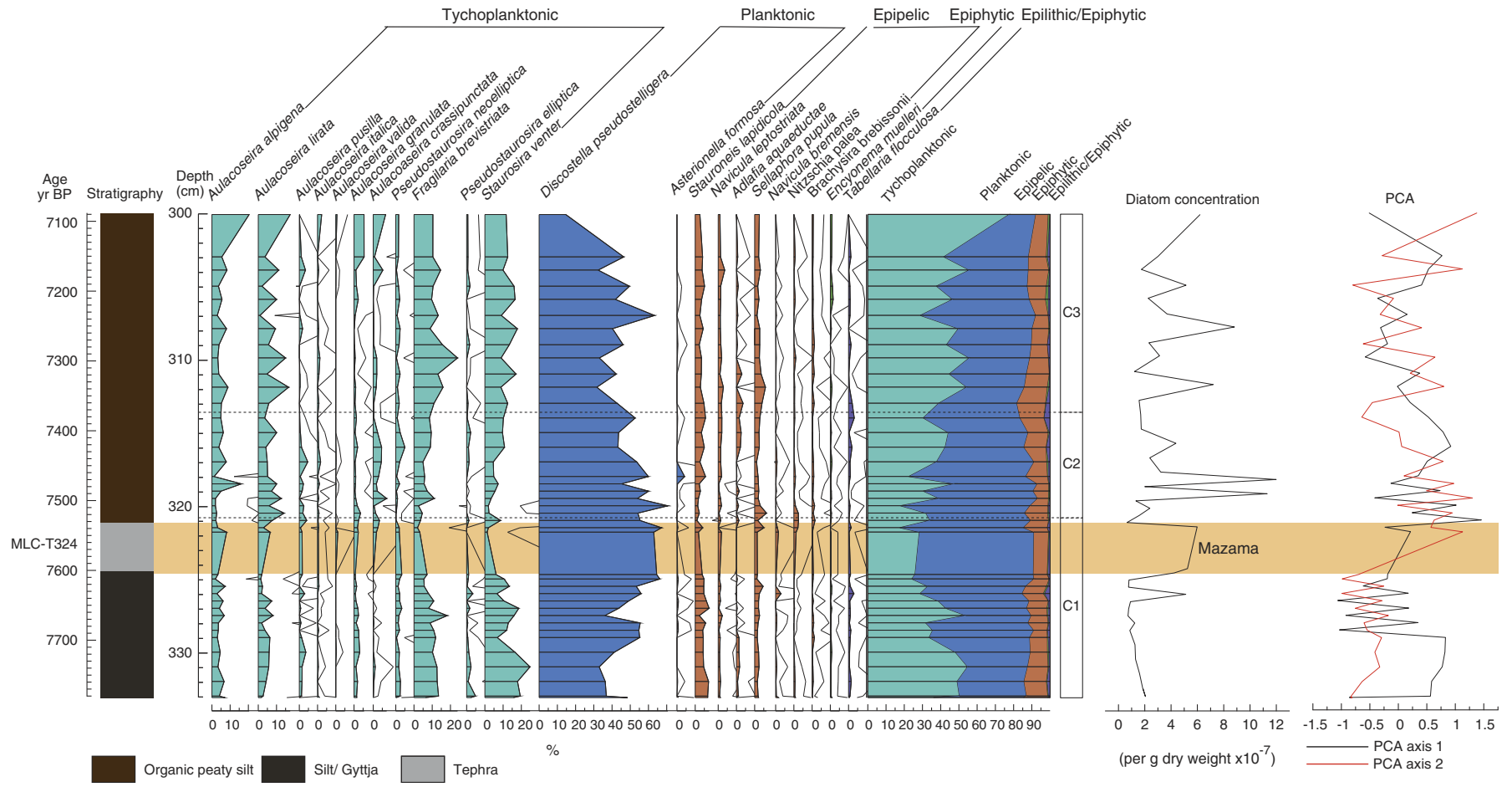


**Figure 5.** Diatom assemblage from Moss Lake central displaying the lithology, percentage of diatoms (with 10x exaggeration), summary diagram, diatom zonation, diatom concentration and PCA axis 1 and 2. The shaded bar represents the location of the Mazama tephra (MLC-T324), also labeled.



**Table 2.** Summary of the diatom assemblage from Moss Lake central (MLC) and Moss Lake fringe (MLF) and their associated zones.

Zone	Depth (cm)	Diatom description	Diatom concentration
MLC			
C3	316.5	<i>Discotella pseudostelligera</i> decrease to 50% but remain dominant. Tycho planktonic species dominate the benthic community (up to 50%).	Variable ( $2 \times 10^8$ – $10 \times 10^7$ per g dry weight).
C2	325	Planktonic and tycho planktonic species continue to dominate (90%). <i>Aulacoseira crassipunctata</i> appear in greater abundance (10%). <i>Fragilaria brevistriata</i> and <i>Staurosira venter</i> start to increase from 5 to 20%. Epipellic species <i>Nitzschia palea</i> , <i>Navicula bremensis</i> and <i>Sellaphora pupula</i> briefly increase.	Variable ( $1 \times 10^8$ – $13 \times 10^7$ per g dry weight).
C1	340	Planktonic <i>Discotella pseudostelligera</i> dominate (up to 60%). Upon tephra deposition tycho planktonic <i>Aulacoseira</i> species increase but <i>Fragilaria brevistriata</i> and <i>Staurosira venter</i> decrease.	Increases upon tephra deposition.
MLF			
F2	156.8	Epipellic species become increasingly important, especially <i>Brachysira brebissonii</i> , <i>Craticula halophila</i> and <i>Nitzschia palea</i> , which increase during tephra deposition. Epiphytic species modestly decline following tephra deposition. Tycho planktonic species decrease after tephra deposition; <i>Staurosira venter</i> nearly disappears.	Low, with a maximum of $1 \times 10^8$ per g dry weight.
F1	160	Tycho planktonic species fluctuate from 10 to 50%, decreasing just before tephra deposition. Epiphytic species dominate just before and upon tephra deposition (~40%). <i>Discotella pseudostelligera</i> briefly appears before tephra deposition and declines towards the top of the zone. <i>Tabellaria flocculosa</i> increases just before tephra deposition, then declines.	Variable ( $0.5 \times 10^8$ – $7 \times 10^8$ per g dry weight).

deposition sample scores show a steady, increasing trend reverting to scores similar to those of the pre-tephra assemblage but not fully back to baseline conditions. Positive sample scores are driven by *Aulacoseira alpigena*, *Staurosira venter*, and *Aulacoseira lirata*. The negative sample scores are driven by *Brachysira brebissonii*, *Frustulia rhomboides*, *Craticula halophila*, and *Navicula bremensis*.

### Partial Redundancy Analysis

For MLC, partial RDA analyses (Table 3) revealed tephra to have a significant unique effect on the diatom assemblages in model 1, but not in models 2 and 3. Depth (directional change) had a significant unique effect in all analyses. LOI also had a significant unique effect except in MLC model 1 (Table 3).

For MLF, the second model was applied to the dataset. In this model, tephra was not significant, but depth and LOI had significant unique effects explaining 37.7% and 15.4% of the variance, respectively.

For MLC, the first model used an exponential decay rate of 0.8, assuming a 500-year recovery period, with most recovery having happened within 200–250 years. This model reported tephra to have a significant unique effect on the diatom assemblage, explaining 11.2% of the variance. Depth also had a significant unique effect, explaining a further 10.6% of the variance. The second model used an exponential decay rate of 0.5, assuming a 200-year recovery period, with most recovery having happened within 100 years. In this model tephra was not significant but depth and LOI indicated significant unique effects explaining 12.7% and 9.1% of the

variance, respectively. The third model assumes a recovery period of 80 years, with most recovery having happened within 20 years, through the application of a decay rate of 0.1, and gave similar results to model 2, with tephra having no significant unique effect on the diatom assemblage but depth and LOI having a significant unique effect, explaining 12.6% and 11.3% of the variance, respectively (Table 3).

### DISCUSSION

Analysis of the diatoms from MLF and MLC clearly illustrates two very different assemblages, with a low proportion of planktonic taxa in MLF (Fig. 6) compared to MLC (Fig. 5) consistent with shallow and deeper lake-water systems, respectively, at the time of the climactic eruption of Mount Mazama. The response to tephra deposition may therefore be expected to differ between the two locations. The species mix confirms that Moss Lake is an oligotrophic, low-alkalinity system with high proportions of *Aulacoseira* taxa and *Brachysira brebissonii*, indicating sensitivity to impacts associated with acidification and/or changes in the nutrient status. The DCA gradients in both data sets for MLF and MLC had lengths of 1.1 and 0.7 SD units respectively, which suggests limited turn-over within the diatom assemblage (Lepš and Smilauer, 2014). However, changes are observed around the time of tephra deposition, with MLC displaying a decline of *Discostella pseudostelligera* and increases of *Aulacoseira* species, and MLF displaying notable decreases of *Aulacoseira* species and epiphytic taxa and increases of

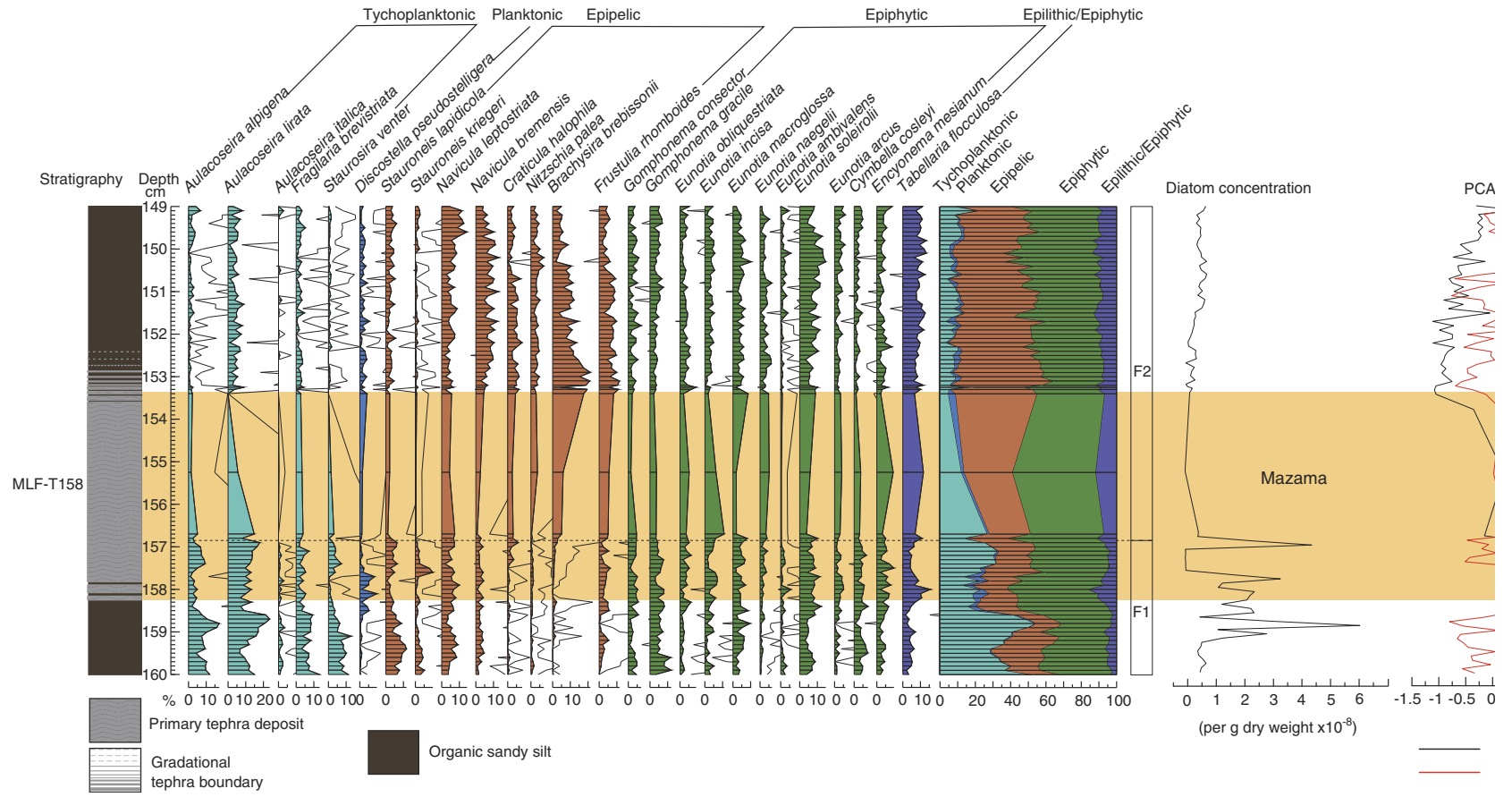


**Figure 6.** (color online) Diatom assemblage from Moss Lake fringe displaying the lithology, percentage of diatoms (with 10x exaggeration), summary diagram, diatom zonation, diatom concentration and PCA axis 1 and 2. The shaded bar represents the location of the Mazama tephra (MLF-T158), also labeled.

**Table 3.** Results of partial redundancy analysis of the diatom stratigraphical data sets of Moss Lake central (MLC) and Moss Lake fringe (MLF), reporting the unique effects and their significance. Those in **bold** are significant. Diatom species with an abundance of >5% or present in at least 10 samples was used in the analysis.

Variable	Tephra	Depth	LOI
Co-variables	Depth + LOI	Tephra + LOI	Tephra + Depth
<b>MLF</b>			
Unique effect (%)	3.6	<b>37.7</b>	<b>15.4</b>
Significance of unique effect	0.204	<b>0.01</b>	<b>0.031</b>
<b>MLC model 1</b>			
Unique effect (%)	<b>11.2</b>	<b>10.6</b>	6.1
Significance of unique effect	<b>0.02</b>	<b>0.02</b>	0.103
<b>MLC model 2</b>			
Unique effect (%)	7.1	<b>12.7</b>	<b>9.1</b>
Significance of unique effect	0.059	<b>0.037</b>	<b>0.048</b>
<b>MLC model 3</b>			
Unique effect (%)	4.5	<b>12.6</b>	<b>11.3</b>
Significance of unique effect	0.252	<b>0.046</b>	<b>0.031</b>

epipellic taxa, in particular *Brachysira brebissonii*. The partial RDA analyses for MLF and models 2 and 3 for MLC revealed that tephra from Mount Mazama overall had no unique significant effect on the diatom assemblages. Model 1 for MLC, however, was the only model indicating a significant unique effect (11.2%) of tephra deposition independent of variation in depth or LOI. Importantly, all of the other models for both MLF and MLC indicate that depth (directional change) had the most significant unique effect on the diatom assemblage (MLF, 37.7%; MLC, 10.6–12.7%) with LOI also having a significant influence (MLF, 15.5%; MLC, 9.1–11.3%).

There is therefore evidence of a tephra effect from the diatom analyses, supported by model 1 of the partial RDA for MLC. The evidence for this tephra effect is not consistent between the two cores, however, or between the different models from MLC. Notably, the partial RDA shows that the underlying environmental changes (represented by depth and LOI) are more influential on the diatom assemblage than any tephra effects.

Nevertheless, there is evidence for a limited tephra effect and there are several hypotheses regarding the potential nature of tephra impacts on lake ecosystems, all of which have been reported in other tephra impact studies: (1) acidification in response to dry deposition of H<sub>2</sub>SO<sub>4</sub> following tephra deposition (Blinman et al., 1979; Birks and Lotter, 1994; Bradbury et al., 2004); (2) change in the nutrient status of the lake following tephra deposition (Barker et al., 2003; Telford et al., 2004); and (3) habitat change following tephra deposition (Brant and Bahls, 1995; Telford et al., 2004).

### Tephra and acidification

It is important to explore the acidification hypothesis, as this is one of the most commonly reported impacts of tephra

deposition (Blinman et al., 1979; Birks and Lotter, 1994; Bradbury et al., 2004). In MLF (and to a lesser extent MLC), increases of *Brachysira brebissonii*, *Tabellaria flocculosa*, *Frustulia rhomboides*, and *Eunotia naegeli* potentially support the acidification hypothesis, as these are acid indicators (Anderson and Renberg, 1992; Fránková et al., 2009) and the declines of the more acid-sensitive *Fragilaria brevistriata* and *Staurosira venter* are also consistent with an acidification event (Anderson and Renberg, 1992). Importantly, however, the diatom response in MLF across all taxa is not consistent with acidification. For example, *Craticula halophila* increases significantly after tephra deposition and prefers alkaline conditions (Round et al., 1990).

Similarly, the diatom data from MLC could be interpreted as showing support for the acidification hypothesis, due to the significance of model 1, and associated changes in *Fragilaria brevistriata* and *Staurosira venter* consistent with increased acidity following tephra deposition. The associated increases in *Nitzschia palea*, *Aulacoseira* species, and *Discostella pseudostelligera*, however, are counter to expected floristic trends following acidification, as they should decrease with increased acid loading (Anderson and Renberg, 1992; Saros and Anderson, 2015). We therefore find no clear evidence of post-tephra acidification in this oligotrophic lake.

### Tephra and nutrient status

The increase of *Aulacoseira* taxa in MLC is consistent with a change in nutrient status, as *Aulacoseira* taxa thrive under silica-rich conditions (Thwaites, 1848; Abella, 1988; Caballero et al., 2006). The increase of silica at that time is most likely to be from tephra deposition, which also prevents the regeneration of nutrients such as phosphorus, as it creates an impermeable barrier over the lakes sediment (Barker et al., 2000, 2003). The reduction of phosphorous may have been a

**Table 4.** The percentage variation of the diatoms indicates which species are most influenced by the variables. The +/- signs mean the species had either a positive or negative relationship with that particular variable.

% Variation of response variable (diatoms)		
Tephra	Depth	LOI
MLF		
<i>Eunotia obliquistriata</i> (+7.8), <i>Eunotia macroglossa</i> (-7.8), <i>Stauroneis lapidicola</i> (-7.5), <i>Eunotia arcus</i> (+6.6), <i>Navicula bremensis</i> (-5.1)	<i>Staurosira venter</i> (+56.2), <i>Nitzschia palea</i> (-55.2), <i>Brachysira brebissonii</i> (-50.2), <i>Tabellaria flocculosa</i> (-47.0), <i>Aulacoseira lirata</i> (+42.6)	<i>Aulacoseira alpigena</i> (+23.1), <i>Brachysira brebissonii</i> (-18.5), <i>Gomphonema gracile</i> (+17.5), <i>Frustulia rhomboides</i> (-17.0), <i>Stauroneis kreigeri</i> (+13.6)
MLC model 1		
<i>Staurosira venter</i> (-65.3), <i>Fragilaria brevistriata</i> (-47.5), <i>Aulacoseira crassipunctata</i> (+44.9), <i>Nitzschia palea</i> (+36.0), <i>Discostella pseudostelligera</i> (+31.1)	<i>Aulacoseira crassipunctata</i> (-29.8), <i>Aulacoseira lirata</i> (-15.3), <i>Discostella pseudostelligera</i> (+15.2), <i>Aulacoseira alpigena</i> (-7.8)	<i>Aulacoseira crassipunctata</i> (-13.2), <i>Aulacoseira granulata</i> (-12.2), <i>Staurosira venter</i> (+6.5)
MLC model 2		
<i>Staurosira venter</i> (-55.8), <i>Aulacoseira crassipunctata</i> (+42.5), <i>Fragilaria brevistriata</i> (-41.6), <i>Aulacoseira valida</i> (+24.5), <i>Nitzschia palea</i> (+23.8)	<i>Aulacoseira crassipunctata</i> (-38.4), <i>Aulacoseira lirata</i> (-19.2), <i>Pseudostaurosira elliptica</i> (+10.0), <i>Staurosira venter</i> (+9.6)	<i>Aulacoseira crassipunctata</i> (-19.8), <i>Staurosira venter</i> (+16.7), <i>Fragilaria brevistriata</i> (+11.8), <i>Aulacoseira granulata</i> (-9.4)
MLC model 3		
<i>Aulacoseira valida</i> (+19.0), <i>Staurosira venter</i> (-17.4), <i>Fragilaria brevistriata</i> (-9.0)	<i>Aulacoseira crassipunctata</i> (-38.0), <i>Aulacoseira lirata</i> (-18.5), <i>Staurosira venter</i> (+12.0), <i>Pseudostaurosira elliptica</i> (+10.6)	<i>Staurosira venter</i> (+26.9), <i>Aulacoseira crassipunctata</i> (-21.7), <i>Fragilaria brevistriata</i> (+19.1), <i>Aulacoseira pusilla</i> (-10.4), <i>Aulacoseira granulata</i> (-10.1)

limiting factor for *Fragilaria brevistriata* and *Staurosira venter* (Abella, 1988), but their generally high tolerance suggests habitat change could have also been influential (Tephra and habitat change). This hypothesis of a nutrient change is also supported by the partial RDA analyses (Table 3) for MLC model 1, as *Aulacoseira crassipunctata* and other *Aulacoseira* taxa respond positively to tephra deposition, and thus the influx of silica. Likewise, *Fragilaria brevistriata* and *Staurosira venter* respond negatively in response to tephra in the partial RDA analyses, which might also suggest a habitat change (Table 4).

### Tephra and habitat change

The floristic changes (increase of *Aulacoseira alpigena* and *Aulacoseira lirata*, decrease of *Fragilaria brevistriata* and *Staurosira venter*, and increase of epipelagic taxa) coincident with tephra deposition in MLC (and MLF, despite the insignificance of tephra) may also suggest an alteration of habitat. The decrease of tychoplanktonic *Fragilaria brevistriata* and *Staurosira venter* and epiphytic taxa are indicative of disturbance and habitat change, as aquatic plants are likely to be adversely affected by tephra deposition due to blanket burial. Although *Fragilaria brevistriata* and *Staurosira venter* are tychoplanktonic (Caballero et al., 2006), they have been reported as epiphytic (Ehrlich, 1995; Stoermer et al., 1996) due to their wide tolerances and tendency to attach themselves to benthic aquatic plants following a disturbance in the tychoplanktonic zone (e.g., tephra deposition). As such, these

species often fluctuate along with aquatic vegetation (Caballero et al., 2006). The local vegetation record from pollen analysis at Moss Lake (Egan et al., 2016), summarized in Figure 7, shows a decrease of *Myriophyllum spicatum* and *Nuphar* due to blanket coverage inhibiting gas exchange and photosynthesis, which would result in a reduction in aquatic vegetation (submerged and emergent). Thus, epiphytic species and *Fragilaria brevistriata* and *Staurosira venter* would decline due to habitat loss (Telford et al., 2004).

The increase of epipelagic taxa, *Staurosira lapidicola*, *Sellaphora pupula*, and *Brachysira brebissonii* further demonstrates habitat change, as these species increase in response to tephra deposition through colonization of the newly deposited tephra (Telford et al., 2004). The increase of *Aulacoseira* taxa also suggests habitat alteration, as they can thrive in turbid waters with low light (Caballero et al., 2006). Partial RDA confirmed tephra to be a significant variable in model 1, with *Staurosira venter* and *Fragilaria brevistriata* responding negatively to the tephra and the potential decline in suitable habitat as a result, and *Nitzschia palea* responding positively to the tephra due to the increase in habitat availability, further supporting this hypothesis.

### Impact summary

In summary, tephra from Mount Mazama had a significant unique effect on the diatom assemblage of the central core (MLC), according to partial RDA model 1, but no significant effect in the fringe core (MLF) or the central core (MLC) when

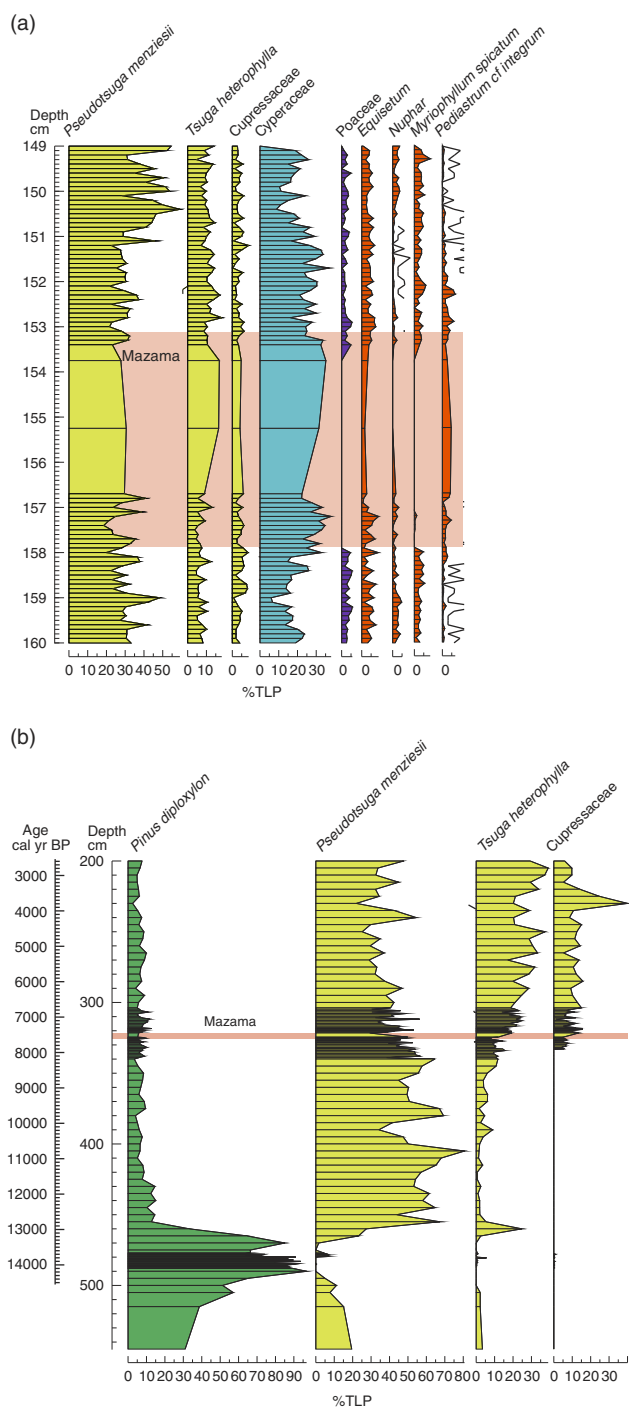


**Figure 7.** Summary pollen diagrams from (a) Moss Lake Fringe (MLF) and (b) Moss Lake Central (MLC). Full pollen diagrams are presented in Egan et al. (2016). Species colored: green, xerophytes; yellow, mesophyte; blue, hydrophyte; orange, spores and aquatics. (For interpretation of the references to color in this figure legend, the reader is referred to the web version of this article.)

applying partial RDA models 2 and 3. There is therefore some evidence of a tephra effect but this is inconsistent. We argue the nature of the effect is a change of habitat conditions and an increase in the Si:P ratio. These impacts lasted for 150–200 years (based on zone data, PCA axis 2, and the age depth

model) to a maximum of 500 years, with most recovery having happened within 200–250 years (based on partial RDA model 1). The transition from diatom zone C2 to C3 reflects the point where the diatom assemblage reverts back to pre-tephra conditions, which is also evident from PCA axis 2 (Fig. 5). This is demonstrated by increases of *Fragilaria brevistriata* and *Stauriosira venter* to baseline levels, reflecting the 150–200 year recovery period. This recovery time period is nearly consistent with partial RDA model 1, which implies a maximum recovery period of 500 years, but with most recovering happening within 200–250 years. Importantly, all partial RDA models indicate that depth and LOI had significant unique effects. This suggests other drivers of change in the aquatic system at the time of the Mazama event, reflecting wider changes in climate, sedimentology, and vegetation.

### Alternative drivers of change

All partial RDA analyses for MLC and MLF (Table 3) indicate that depth (surrogate for directional change) had the most significant unique effect on the diatom assemblage (MLF, 37.7%; MLC, 10.6–12.7%). LOI was also identified as an important variable (MLF, 15.5%; MLC, 9.1–11.3%). Taxa explained by depth in MLF are *Stauriosira venter*, *Nitzschia palea*, *Brachysira brebissonii*, *Tabellaria flocculosa*, and *Aulacoseira lirata* (Table 4). These taxa represent the most notable changes in the MLF diatom assemblage and, although the partial RDA analysis indicates depth to have the greatest significant unique effect, there are a few caveats with the partial RDA analysis that must be highlighted. There is a potential issue with the MLF model, as there was no evidence of recovery, which is what the model assumed. Given the sensitivity of lake fringes, one might have expected a more pronounced impact of tephra here. Instead, depth appears to be the significant variable, but there is a possibility that depth could have been acting as a surrogate for tephra (as there is no evidence of recovery) and, in fact, tephra may be more important than indicated by this model. Despite this, all but one model for MLC indicate an insignificant independent response to tephra deposition, with depth (directional change) being the main driver.

Taxa explained by depth in MLC are *Aulacoseira crassipunctata* and *Aulacoseira lirata* in all models and *Discostella pseudostelligera* in model 1 (Table 4). *Discostella pseudostelligera* are likely to be responding to ongoing climate change as PCA axis 1 (Fig. 5) is representative of short-term environmental change and correlates well with variations in *Discostella pseudostelligera*. Further, Egan (2016) report fluctuations of *Aulacoseira* taxa and *Discostella pseudostelligera* in response to climatic changes at that time. LOI also had a significant unique effect and is likely to reflect the change in sedimentology around the time of Mazama tephra deposition from silty gyttja to organic peaty silt (Fig. 2). This change in sedimentology could potentially be a result of tephra deposition, as it can reduce infiltration and increase surface wetness, potentially creating waterlogged conditions for peaty silt to



develop. As models 2 and 3 for MLC and MLF indicate an insignificant effect of tephra, however, this is unlikely. Alternatively, LOI could be influenced by longer-term environmental change. During the time of tephra deposition, Moss Lake was in a period of transition with an increase of nutrients from both a warmer climate (beginning 8000 cal yr BP until 6500 cal yr BP) and the developing conifer forest ecosystem, particularly *Pseudotsuga menziesii*, *Tsuga heterophylla*, and Cupressaceae, at that time (Egan et al., 2016), summarized in Figure 7b. There is also evidence that during the Holocene the lake was undergoing hydroseral succession in the marginal areas of the lake basin, as evidenced by the increasing LOI and development of silty peats (Fig. 6). These catchment-wide changes allowed longer growing seasons, increased nutrient availability, and increased habitat availability for diatoms, increasing diatom diversity (Egan, 2016). Thus, the addition of tephra may have amplified these changes in nutrient status and hydroseral succession, as the addition of silica into the system would have a positive effect on some diatoms (i.e., *Aulacoseira* taxa), while the tephra itself further increases habitat availability for the epipelagic species and contributes to sediment influx. Given that the partial RDA analyses only indicate that tephra had a significant unique effect in one model, however, it can be concluded that the effect of tephra on the aquatic system of Moss Lake was minimal in relation to underlying environmental trends.

## CONCLUSION

The climatic eruption of Mount Mazama was a major volcanic event in North America during the Holocene. At Moss Lake, up to 50 mm of tephra were deposited. There is some evidence for significant and independent impacts of this tephra on the aquatic ecosystem, but these are not consistent between the central and fringe core locations. Partial RDA analyses indicated that tephra had no unique significant effect on the diatom assemblages of the fringe core location, whereas the partial RDA models for the central core location based on a 500-year maximum recovery period, with most recovery happening with 200–250 years, were significant.

The diatom response recorded in both the shallow- and deep-water lake systems suggests that there was a change in habitat availability with a reduction in tychoplanktonic (particularly *Fragilaria brevistriata* and *Staurosira venter*) and epiphytic taxa and an increase in epipelagic taxa (particularly *Brachysira brebissonii* and *Frustulia rhomboides*). There was also a change in the Si:P ratio, with an increase of *Aulacoseira* taxa recorded in the deep-water lake system. These changes are coincident with the timing of tephra deposition and are also associated with ongoing environmental change within the catchment, with both a warmer climate and the expansion of a conifer forest evidenced by pollen analyses on MLF and MLC. The climate and catchment wide changes could have been amplified by tephra deposition due to the addition of silica contributing to nutrient availability and the sediment (tephra) influx increasing epipelagic habitat availability.

Overall the partial RDA analyses indicate some evidence of an effect, likely to be habitat change, but this is not consistent between the central and fringe core and the tephra impact is not as important as changes in the assemblages caused by underlying environmental trends. There is a natural tendency to equate any coincidental diatom change with the impact of tephra deposition. Without high resolution analyses, cross correlations with multiple cores and other records, and robust statistical analyses, it is difficult to determine how influential tephra is.

## ACKNOWLEDGMENTS

This work was supported by the NERC Radiocarbon Facility NRCF010001 (allocation numbers 1877.1014; 1728.1013). Fieldwork was partially funded by the Royal Geographical Society with IBG (Geographical Club Award Ref. 03.13). We thank Danielle Alderson (The University of Manchester), Douglas H. Clark and Harold N. Wershow (Western Washington University) for assistance in the field.

## SUPPLEMENTARY AND ARCHIVED DATA

All diatom and stratigraphic data are available from <https://doi.pangaea.de/10.1594/PANGAEA.890666>, in addition to the supplementary data already discussed within the manuscript. To view supplementary material for this article, please visit <https://doi.org/10.1017/qua.2018.73>

## REFERENCES

- Abella, S.E., 1988. The effect of Mt. Mazama ashfall on the planktonic diatom community of Lake Washington. *Limnology and Oceanography* 33, 1376–1385.
- Anderson, N.J., Renberg, I., 1992. A paleolimnological assessment of diatom production responses to lake acidification. *Environmental Pollution* 78, 113–119.
- Ayris, P.M., Delmelle, P., 2012. The immediate environmental effects of tephra emission. *Bulletin of Volcanology* 74, 1905–1936.
- Barker, P., Telford, R., Merdaci, O., Williamson, D., Taieb, M., Vincens, A., Gibert, E., 2000. The sensitivity of a Tanzanian crater lake to catastrophic tephra input and four millennia of climate change. *The Holocene* 10, 303–310.
- Barker, P., Williamson, D., Gasse, F., Gibert, E., 2003. Climatic and volcanic forcing revealed in a 50,000-year diatom record from Lake Massoko, Tanzania. *Quaternary Research* 60, 368–376.
- Battarbee, R.W., 1986. Diatom analysis. In: Berglund, B.E. (Ed.), *Handbook of Holocene Palaeoecology and Palaeohydrology*. John Wiley and Sons, Chichester, pp. 527–570.
- Battarbee, R., Kneen, M.J., 1982. The use of electronically counted microspheres in absolute diatom analysis. *Limnology and Oceanography* 27, 184–188.
- Bennett, K.D., 1996. Determination of the number of zones in a biostratigraphical sequence. *New Phytologist* 132, 155–170.
- Bennett, K.D., 2007. Psimpoll and Pscomb programs for plotting and analysis (accessed February 18, 2015). <http://www.chrono.qub.ac.uk/psimpoll/psimpoll.html>.

- Birks, H.J.B., Lotter, A.F., 1994. The impact of the Laacher See Volcano (11 000 yr B.P.) on terrestrial vegetation and diatoms. *Journal of Paleolimnology* 11, 313–322.
- Blackford, J.J., Payne, R.J., Heggen, M.P., de la Riva Caballero, A., van der Plicht, J., 2014. Age and impacts of the caldera-forming Aniakchak II eruption in western Alaska. *Quaternary Research* 82, 85–95.
- Blinman, E., Mehringer, P.J., Sheppard, J.C., 1979. Pollen influx and the deposition of Mazama and Glacier Peak tephra. In: Sheets, P., Grayson, D. (Eds.), *Volcanic Activity and Human Ecology*. Academic Press, London, pp. 393–425.
- Bradbury, P.J., Colman, S.M., Dean, W.E., 2004. Limnological and Climatic Environments at Upper Klamath Lake, Oregon during the past 45 000 years. *Journal of Paleolimnology* 31, 167–188.
- Brant, L., Bahls, L., 1995. Paleoenvironmental impacts of volcanic eruptions upon a diatom community. In: Kocielek, J.P., Sullivan, M.J. (Eds.), *A Century of Diatom Research in North America: A Tribute to the Distinguished Careers of Charles W. Reimer and Ruth Patrick*. Koeltz Scientific, Stuttgart.
- Bronk Ramsey, C., 2014. OxCal V. 4.2 (accessed November 20, 2014). <https://c14.arch.ox.ac.uk/oxcal/OxCal.html>.
- Caballero, M., Vázquez, G., Lozano-García, S., Rodríguez, A., Sosa-Nájera, S., Ruiz-Fernández, A.C., Ortega, B., 2006. Present limnological conditions and recent (ca. 340 yr) palaeolimnology of a tropical lake in the Sierra de Los Tuxtlas, Eastern Mexico. *Journal of Paleolimnology* 35, 83–97.
- Colman, S.M., Bradbury, J., McGeehin, J.P., Holmes, C.W., Edginton, D., Sarna-Wojcicki, A.M., 2004. Chronology of sediment deposition in Upper Klamath Lake, Oregon. *Journal of Paleolimnology* 31, 139–149.
- Dragovich, J.D., Logan, R.L., Schasses, H.W., Walsh, T.J., Lingley, W.S.J., Norman, D.K., Gerstel, W.J., Lapen, T.J., Schuster, J.E., Meyers, K.D., 2002. Geological Map of Washington—Northwest Quadrant. Washington Division of Geology and Earth Resources Geological Map GM-50, scale 1:250,000. Washington Department of Natural Resources, Olympia.
- Egan, J., 2016. *Impact and Significance of Tephra Deposition from Mount Mazama and Holocene Climate Variability in the Pacific Northwest USA*. PhD Thesis, The University of Manchester, Manchester, United Kingdom.
- Egan, J., Fletcher, W.J., Allott, T.E.H., Lane, C.S., Blackford, J.J., Clark, D.H., 2016. The impact and significance of tephra deposition on a Holocene forest environment in the North Cascades, Washington, USA. *Quaternary Science Reviews* 137, 135–155.
- Egan, J., Staff, R.A., Blackford, J., 2015. A revised age estimate of the Holocene Plinian eruption of Mount Mazama, Oregon using Bayesian statistical modelling. *The Holocene* 25, 1054–1067.
- Ehrlich, A., 1995. *Atlas of the Inland-water Diatom Flora of Israel*. The Geological Survey of Israel and the Israel Academy of Sciences and Humanities, Jerusalem.
- Fránková, M., Bojková, J., Pouličková, A., Hájek, M., 2009. The structure and species richness of the diatom assemblages of the Western Carpathian spring fens along the gradient of mineral richness. *Fottea* 9, 355–368.
- Heinrichs, M.L., Walker, I.R., Mathewes, R.W., Hebda, R.J., 1999. Holocene chironomid-inferred salinity and paleovegetation reconstruction from Kilpoola Lake, British Columbia. *Géographie physique et Quaternaire* 53, 211–221.
- Hickman, M., Reasoner, M.A., 1994. Diatom responses to late Quaternary vegetation and climate change, and to deposition of two tephra in an alpine and a sub-alpine lake in Yoho National Park, British Columbia. *Journal of Paleolimnology* 11, 173–188.
- Hill, M., Gauch, H., 1980. Detrended correspondence analysis: an improved ordination technique. *Vegetatio* 42, 47–58.
- Kelly, M.G., Bennion, H., Cox, E.J., Goldsmith, B., Jamieson, J., Juggins, S., Mann, D.G., Telford, R.J., 2005. Craticula. Common freshwater diatoms of Britain and Ireland: an interactive key (accessed November 10, 2015). Environment Agency, Bristol. <http://craticula.ncl.ac.uk/EADiatomKey/html/index.html>.
- Krammer, K., Lange-Bertalot, H., 1991. *Süßwasserflora von Mitteleuropa vol. 2/4 Bacillariophyceae*. Gustav Fischer Verlag, Stuttgart.
- Krammer, K., Lange-Bertalot, H., 1999a. *Süßwasserflora von Mitteleuropa vol. 2/1 Bacillariophyceae*. Spektrum Akademischer verlag GmbH, Berlin.
- Krammer, K., Lange-Bertalot, H., 1999b. *Süßwasserflora von Mitteleuropa vol 2/2 Bacillariophyceae*. Spektrum Akademischer verlag GmbH, Berlin.
- Lallement, M., Macchi, P.J., Vigliano, P., Juarez, S., Rechencq, M., Baker, M., Bouwes, N., Crowl, T., 2016. Rising from the ashes: Changes in salmonid fish assemblages after 30 months of the Puyehue-Cordon Caulle volcanic eruption. *The Science of the Total Environment* 541, 1041–1051.
- Lepš, J., Smilauer, P., 2014. *Multivariate Analysis of Ecological Data Using CANOCO 5*. 2nd ed. Cambridge University Press, Cambridge.
- Lotter, A.F., Anderson, N.J., 2012. Limnological Responses to Environmental Changes at Inter-annual to Decadal Time-scales. In: Birks, H.J.B., Lotter, A.F., Juggins, S., Smol, J.P. (Eds.), *Tracking Environmental Change Using Lake Sediments, Developments in Paleoenvironmental Research* 5. Springer, New York, pp. 557–578.
- Lotter, A.F., Birks, H., 1993. The impact of the Laacher See tephra on terrestrial and aquatic ecosystems in the Black Forest, southern Germany. *Journal of Quaternary Science* 8, 263–276.
- Mass, C.F., Portman, D.A., 1989. Major volcanic eruptions and climate: a critical evaluation. *Journal of Climate* 2, 566–593.
- McCormick, M.P., Thomason, L.W., Trepte, C.R., 1995. Atmospheric effects of the Mt Pinatubo eruption. *Nature* 373, 399–404.
- Orlaci, L., 1966. Geometric models in ecology: I. The theory and application of some ordination methods. *Journal of Ecology* 54, 193–215.
- Payne, R., Blackford, J., 2008. Distal volcanic impacts on peatlands: palaeoecological evidence from Alaska. *Quaternary Science Reviews* 27, 2012–2030.
- Payne, R.J., Egan, J., 2017. Using palaeoecological techniques to understand the impacts of past volcanic eruptions. *Quaternary International* (in press).
- Porter, S.C., Swanson, T.W., 1998. Radiocarbon age constraints on rates of advance and retreat of the Puget Lobe of the Cordilleran Ice Sheet during the last glaciation. *Quaternary Research* 50, 205–213.
- Power, M.J., Whitlock, C., Bartlein, P.J., 2011. Postglacial fire, vegetation, and climate history across an elevational gradient in the Northern Rocky Mountains, USA and Canada. *Quaternary Science Reviews* 30, 2520–2533.
- Pyne-O'Donnell, S.D., Hughes, P.D., Froese, D.G., Jensen, B.J., Kuehn, S.C., Mallon, G., Amesbury, M.J., Charman, D.J., Daley, T.J., Loader, N.J., Mauquoy, D., 2012. High-precision ultra-distal Holocene tephrochronology in North America. *Quaternary Science Reviews* 52, 6–11.
- Rao, C., 1964. The use and interpretation of principal component analysis in applied research. *Sankhyā: The Indian Journal of Statistics, Series A* 26, 329–358.

- Reimer, P., Bard, E., Bayliss, A., Beck, J.W., Blackwell, P.G., Bronk Ramsey, C., Buck, C.E., et al., 2013. IntCal13 and marine13 radiocarbon age calibration curves 0–50,000 years cal BP. *Radiocarbon* 55, 1869–1887.
- Renberg, I., 1990. A procedure for preparing large sets of diatom slides from sediment cores. *Journal of Paleolimnology* 4, 87–90.
- Rose, W.I., Durant, A.J., 2009. Fine ash content of explosive eruptions. *Journal of Volcanology and Geothermal Research* 186, 32–39.
- Round, F., Crawford, R., Mann, D., 1990. *The Diatoms: Biology and Morphology of the Genera*. Cambridge University Press, Cambridge.
- Saros, J.E., Anderson, N.J., 2015. The ecology of the planktonic diatom *Cyclotella* and its implications for global environmental change studies. *Biological reviews of the Cambridge Philosophical Society* 90, 522–541.
- Spaulding, S., 2014. Diatoms of the United States (accessed October 31, 2014). <http://westerndiatoms.colorado.edu/>.
- Staff, R.A., Bronk Ramsey, C., Bryant, C.L., Brock, F., Payne, R.L., Schlolaut, G., Marshall, M.H., et al., 2011. New  $^{14}\text{C}$  determinations from Lake Suigetsu, Japan: 12,000 to 0 cal BP. *Radiocarbon* 53, 511–528.
- Stoermer, E.F., Emmert, G., Julius, M.L., Schelske, C.L., 1996. Paleolimnologic evidence of rapid recent change in Lake Erie's trophic status. *Canadian Journal of Fisheries and Aquatic Sciences* 53, 1451–1458.
- Stoffel, M., Khodri, M., Corona, C., Guillet, S., Poulain, V., Bekki, S., Guiot, J., et al., 2015. Estimates of volcanic-induced cooling in the Northern Hemisphere over the past 1,500 years. *Nature Geoscience* 8, 784–788.
- Stone, J.R., 2005. *A High-Resolution Record of Holocene Drought Variability and the Diatom Stratigraphy of Foy Lake, Montana*. PhD Thesis, University of Nebraska, Lincoln.
- Telford, R., Barker, P., Metcalfe, S., Newton, A., 2004. Lacustrine responses to tephra deposition: examples from Mexico. *Quaternary Science Reviews* 23, 2337–2353.
- ter Braak, C., Prentice, I., 1988. *A Theory of Gradient Analysis*. Academic Press Inc, London.
- ter Braak, C., Šmilauer, P., 2012. *Canoco Reference Manual and User's Guide: Software for Ordination, Version 5.0*. Microcomputer Power, Ithaca.
- Thwaites, G.H.K., 1848. XVI—Further observations on the Diatomaceæ; with descriptions of new genera and species. *Journal of Natural History Series 2* 1, 161–172.
- Zdanowicz, C.M., Zielinski, G.A., Germani, M.S., 1999. Mount Mazama eruption: calendrical age verified and atmospheric impact assessed. *Geology* 27, 621–624.
- Zielinski, G.A., 2000. Use of paleo-records in determining variability within the volcanism–climate system. *Quaternary Science Reviews* 19, 417–438.